PHYSICAL REVIEW C VOLUME 23, NUMBER 2 FEBRUARY 1981

Thermal flucatuations in a classical theory with shape degrees of freedom for heavy ion collisions

S. K. Samaddar,* D. Sperber, and M. Zielińska-Pfabe†
Department of Physics, Rensselaer Polytechnic Institute, Troy, New York

M. I. Sobel
Department of Physics, Brooklyn College, Brooklyn, New York

S. I. A. Garpman
The Niels Bohr Institute, Copenhagen, Denmark
(Received 10 March 1980)

We use a classical dynamical theory with shape degrees of freedom to describe deep inelastic scattering of heavy ions, and include thermal fluctuations by means of the Fokker-Planck equation. The degrees of freedom allow for neck formation, mass transfer, and stretching of the two-nucleus system. Inertias are calculated for these degrees of freedom, and dissipative and conservative forces are used. Fluctuations are calculated by considering the second moments of the distribution and determining a temperature from the excitation energy at each time. We calculate distributions in final energy, angle, charge, and mass, including some double differential cross sections. Results are in good agreement with data.

[NUCLEAR REACTIONS Classical dynamical model, shape degrees of freedom, Fokker-Planck equation, thermal fluctuations; angular, energy, mass, and charge distributions are calculated for the reactions $^{209}Bi + ^{84}Kr$, $^{209}Bi + ^{136}Xe$, and $^{197}Au + ^{63}Cu$.]

I. INTRODUCTION

In this paper we present a classical theory which accounts for the observed properties of strongly damped collisions. In particular, we show that the model explains very well (a) the angular distribution of the projectile-like fragment, (b) the energy loss, (c) the width of the mass distribution, (d) the mass drift in most reactions, and (e) the correlation between energy loss and the width of the mass distribution.

The theory is based on a trajectory calculation. Trajectory calculations have been shown to reproduce qualitatively the properties of strongly damped collisions.[1] However, simple trajectory calculations always predict (i) a too narrow angular distribution and (ii) no mass distribution or mass drift. Furthermore, they do not allow for the very high observed energy loss below the Coulomb barrier of two touching spheres. Finally, simple trajectory calculations require a number of adjustable parameters to fit the data.

It is clear that in order to obtain a wide mass or charge distribution one has to include thermal and quantum fluctuations. During the earliest stages of the interaction between the ions, quantum fluctuations may be significant. However, in collisions that are strongly damped one sees primarily smooth distributions, with no evidence of interference effects characteristic of quantum fluctuations, and so it is likely that thermal fluctuations dominate. It has been shown[2] that by describing the time evolution of the mass or charge asymmetry degrees of freedom by a Fokker-Planck equation, one can explain very well the charge or mass drift and distribution. However, such a nondynamical calculation cannot reproduce the angular distribution or the energy loss. One way to incorporate both the dynamical and thermal aspects of strongly damped collisions is to include random transfer through the neck region during the course of a trajectory calculation.[3] In such a model one integrates the equations of motion many times for a selected number of impact parameters and obtains the wide distributions. This model accounts very well for the mass or charge distribution and drift. Its two main shortcomings are (i) that the time evolution of the neck is treated nondynamically, and (ii) that the very considerable energy losses, below the Coulomb barrier of two touching spheres, are not accounted for.

In order to remedy the second shortcoming one has to introduce collective degrees of freedom as soon as the ions touch, and to study the time evolution of these degrees of freedom. Such a model has recently been discussed.[4] The time evolution of the collective degrees of freedom has been studied dynamically. The three degrees of free-

dom are (i) the size of the neck, (ii) the mass asymmetry, and (iii) stretching. The model was used to determine (i) the deflection function, (ii) the mass drift (this is possible since mass asymmetry is one of the degrees of freedom), and (iii) the energy loss. However, such a generalized trajectory does not include thermal fluctuations and therefore does not account for the widths of the distribution in angle, energy, charge, and mass.

We have seen that trajectory calculations have been generalized in two different ways: (i) to include thermal fluctuations, and (ii) to include collective deformation. The most general version of a classical trajectory calculation would include both collective deformations and thermal fluctuations. Such a model is proposed in this paper.

The collective deformations are the same as in the previous work.[4] Thermal fluctuations can be introduced in three different ways. First, one can use a Monte Carlo model and allow random transfer. Such a model, with many degrees of freedom is not practical from a computational point of view. Alternatively, one can solve the full Fokker-Planck equation for the deep (collective) phase. This is a partial differential equation with six variables besides the time, and is also not computationally practical. Finally, one can use the Fokker-Planck equation, but study only the first two moments of the distribution. This approach has been adopted here.

Recently Ngô and Hofmann[5] have shown that if the distribution is narrow then it takes the form of a Gaussian which can be described entirely by its first and second moments; and the partial differential Fokker-Planck equation can be replaced by first order coupled differential equations in time for these moments. We have adapted these equations to the study of the collective coordinates. It is not surprising that the equations for the first moments are identical to the Euler-Lagrange equations without thermal fluctuations. The information obtained from the time evolution of the first and second moments allows us the determination of the widths of the angular distribution, mass or charge distribution, and energy distribution.

The coefficients in the coupled linear differential equations require knowledge of the inertial parameters, the frictional parameters, and the conservative potential as well as their derivatives with respect to collective variables. The mathematical details of calculating these parameters are discussed in Ref. 4. Here we will recall that (a) the inertial parameters are evaluated assuming incompressible irrotational flow; (b) the frictional parameters are evaluated assuming one-body dissipation using the wall formula; (c) the potential energy is evaluated assuming that the nuclear potential is proportional to the surface area; and (d) the Coulomb potential is obtained by numerical integration over the charge distribution of the two-nucleus system. These quantities have been calculated previously[4] (when thermal fluctuations have been excluded).

It is important to determine if the collective shape deformations and associated fluctuations occur for all trajectories or only for the deeper trajectories. We therefore consider two cases: (i) all angular momenta undergoing deep inelastic scattering enter the phase of collective deformation; and (ii) only for those angular momenta for which two ions touch, the collective phase and the associated fluctuations are established. We find that the latter model agrees better with experiment. This is reasonable as it may be argued that collective shape deformations and fluctuations develop only for small and intermediate impact parameters, for peripheral trajectories the deep phase is never reached.

We apply the model to the study of the reactions[6-8] ^{209}Bi + ^{84}Kr at 600 MeV, ^{209}Bi + ^{136}Xe at 1130 MeV, and ^{197}Au + ^{63}Cu at 443 MeV. The theory is outlined in Sec. II. Comparison with experiment and discussion are found in Sec. III.

II. THEORY

The classical dynamical model is described in Ref. 4, and here we give a brief summary. The collision occurs in three phases: In the initial phase the ions are sufficiently separated so that no distortion of the nuclear shape takes place, and the system can be described by the relative coordinate between the centers of mass of the two nuclei. The interaction is given by the Coulomb potential, and, when the ions are closer, the proximity potential[9] and the proximity friction[10] are included.

When the distance between the centers of the ions reaches a certain separation, r_{coll}, the deep phase is established and the dinuclear system is then described by collective degrees of freedom. The distance r_{coll} corresponds to the point where the decrease in potential energy which occurs on entering the deep phase is maximum. The generalized coordinates are three variables which describe the shape of the two-nucleus system; the system moves with constant volume. The choice of collective degrees of freedom is given in Ref. 4; it allows for an approximation to two tangent spheres, for neck formation, for mass transfer (which means one sphere increases in volume while the other decreases), for stretching apart

toward a scission point, and for formation of a single sphere or spheroid (fusion of the ions). In making the transition to the collective coordinates, matching conditions were applied to determine the initial values of the generalized coordinates and their velocities. Two models were considered: the "heat" model in which all the kinetic energy of the initial phase is lost (transforms to heat) so that the collective coordinates start with zero velocities; the "kinetic" model in which all the kinetic energy remains in the collective modes. The difference between the models in the trajectory calculation is not great, and in the present paper we use only the kinetic model. Furthermore, there is one free parameter in the initial coordinate values, and this is taken to be the radius of the neck h. We choose h, as in Ref. 4, so that the scattering angle at the center of the distribution agrees with the experimental value.

During the deep phase the equations of motion are solved using the wall formula for dissipation and using collective inertias derived from the assumption of irrotational incompressible flow.

Finally the system either approaches a single spheroid, or stretches apart to a scission point. In the former case we say fusion has occurred. (We do not have any fusion for the systems studied in this paper, although the model does predict fusion for some lighter systems.[11]) In the latter case a scission criterion is applied, based on the idea that the repulsive Coulomb and centrifugal forces exceed the attractive tensile force across the neck region.[12] This scission criterion leads to the existence of a minimum possible value of h, such that if $h < h_{\min}$ then the system will immediately scission, and not enter the deep phase for all L's up to $L_{\max}$. After scission the ions travel to infinity under the influence of the Coulomb force, and we calculate the final scattering angle, energy, and mass division.

Tangential friction is simulated by imposing the sticking condition at the beginning of the deep phase. The charge transfer degree of freedom is treated by assuming rapid charge equilibration for a given mass division.[13]

If the system is thought of as being in contact with a heat bath of temperature τ then one obtains a distribution W in the classical coordinates and momenta. The equation for W in phase space is the Chandrasekhar generalization of the Fokker-Planck equation.[14] We wish to discuss the form of this equation for a general classical system, described by coordinates, β_i; $i = 1, 2, \ldots$. First we write, for completeness, the classical trajectory equations for the deep phase. Let the kinetic energy and the Rayleigh dissipation function be T and R, respectively, where

$$T = \tfrac{1}{2} \sum_{ij} T_{ij} \dot{\beta}_i \dot{\beta}_j ,$$
$$R = \tfrac{1}{2} \sum_{ij} R_{ij} \dot{\beta}_i \dot{\beta}_j , \tag{2.1}$$

and let the potential energy be V. Here T_{ij} and R_{ij} are the inertia tensor and the friction tensor, respectively. The quantities T, R, and V are functions of the β's. It is convenient to express the fluctuation equations in terms of the momenta instead of the velocities, and to write equations for the classical path in Hamiltonian form; and so we introduce the canonical momenta defined by

$$p_i = \frac{\partial \mathcal{L}}{\partial \dot{\beta}_i} \tag{2.2}$$

where $\mathcal{L} = T - V$ is the Lagrangian. Then the classical trajectory is given by

$$\frac{d\beta_i}{dt} = \sum_j U_{ij} p_j , \tag{2.3}$$

$$\frac{dp_i}{dt} = -\tfrac{1}{2} \sum_{jk} \frac{\partial U_{jk}}{\partial \beta_i} p_j p_k - \frac{\partial V}{\partial \beta_i} - \sum_j R_{ij} \frac{d\beta_j}{dt} , \tag{2.4}$$

where $U = T^{-1}$ is the inverse inertia matrix. In Eq. (2.4) the $\dot{\beta}_j$ can be replaced according to Eq. (2.3).

The distribution function $W(\beta, p; t)$ obeys the equation

$$\frac{\partial W}{\partial t} + \sum_i \frac{\partial}{\partial \beta_i} \left(\frac{d\beta_i}{dt} W \right) + \sum_i \frac{\partial}{\partial p_i} \left(\frac{dp_i}{dt} W \right) = \tau \sum_{ij} \frac{\partial}{\partial p_i} \frac{\partial}{\partial p_j} (R_{ij} W) . \tag{2.5}$$

Here again, one substitutes from Eqs. (2.3) and (2.4) into the second and third terms to obtain an equation in p, β, and t. Inclusion of the temperature-dependent term on the right side generates the thermal fluctuations.

For the temperature we use

$$\tau = (E^*/a)^{1/2} ,$$

where E^* is the dynamically calculated time-dependent excitation energy. Specifically we may write

$$E^* = E_{\text{c.m.}} + \mathcal{U}_1 + \mathcal{U}_2 - (E_{\text{rot}} + \mathcal{U} + K) ,$$

where $E_{\text{c.m.}}$ is the incident center of mass energy; $\mathcal{U}_1$ and $\mathcal{U}_2$ are liquid drop potential energies of projectile and target before the collisions; $\mathcal{U}$ and K are the instantaneous liquid drop potential energy and collective kinetic energy of the fused system; and E_{rot} is the rotational energy of the fused system. In other words, the collective energy is calculated explicitly from the known shape and inertial parameters, and all other energies

are assumed to be in the intrinsic coordinates.

In our calculation we take $a=(A_1+A_2)/10\ \mathrm{MeV}^{-1}$; i.e., the system is treated as a Fermi gas with temperature small as compared to the Fermi energy. We are assuming here that the system will not cool significantly by particle evaporation during the deep phase.

We are interested in heavy ion scattering for which the classical trajectories have meaning, and therefore we expect distributions which are fairly narrow around the classical path. This does not require that the total distribution be narrow. Rather the distribution for each incident angular momentum, or impact parmeter, should be narrow. The final distribution is obtained by summing over all angular momenta.

The condition that the distribution be narrow is that τ be small compared to other energies in the problem. In this case we may assume that the distribution is adequately characterized by its first and second moments. We define these, following the notation of Ref. 5, as follows:

$$\beta_i^c=\int d\Gamma\,\beta_i\,,$$

$$p_i^c=\int d\Gamma\,p_i\,,$$

$$\omega_{ij}=\tfrac{1}{2}\int d\Gamma(p_i-p_i^c)(p_j-p_j^c)\,, \tag{2.6}$$

$$\chi_{ij}=\tfrac{1}{2}\int d\Gamma(\beta_i-\beta_i^c)(\beta_j-\beta_j^c)\,,$$

$$\psi_{ij}=\tfrac{1}{2}\int d\Gamma(p_i-p_i^c)(\beta_j-\beta_j^c)\,,$$

where $d\Gamma=W d\beta_1\ldots dp_1\ldots$. One then verifies that β_i^c and p_i^c obeys Eqs. (2.3) and (2.4), respectively. Equations for the time variations of ω, ψ, and χ are derived by multiplying Eq. (2.5) by $(p_i-p_i^c)\,(p_j-p_j^c)$, for example, and then integrating by parts. The result is given in Ref. 5, but we repeat it here for completeness and also because there is one term which we find below that has been omitted in that paper.

$$\frac{d\omega_{ij}}{dt}=-\Bigg[\sum_{kl}\left(p_k^c\frac{\partial U_{lk}}{\partial\beta_i}\omega_{jl}+R_{ik}U_{lk}\omega_{lj}\right)+\sum_k C_{ik}\psi_{jk}+\sum_{klm}\left(\tfrac{1}{2}p_k^cp_l^c\frac{\partial^2U_{kl}}{\partial\beta_m\partial\beta_i}+p_l^cR_{ik}\frac{\partial U_{lk}}{\partial\beta_m}+p_l^c\frac{\partial R_{ik}}{\partial\beta_m}U_{kl}\right)\psi_{jm}\Bigg]+\{i\rightleftharpoons j\}+R_{ij}\tau\,, \tag{2.7a}$$

$$\frac{d\psi_{ij}}{dt}=\sum_{kl}\left[p_k^c\left(\frac{\partial U_{jk}}{\partial\beta_l}\psi_{il}-\frac{\partial U_{lk}}{\partial\beta_i}\psi_{lj}\right)-R_{ik}U_{lk}\psi_{lj}\right]+\sum_k(U_{kj}\omega_{ki}-C_{ik}\chi_{kj})-\sum_{klm}\left(\tfrac{1}{2}p_k^cp_l^c\frac{\partial^2U_{kl}}{\partial\beta_m\partial\beta_i}+R_{ik}p_l^c\frac{\partial U_{lk}}{\partial\beta_m}\right)\chi_{mj}\,, \tag{2.7b}$$

$$\frac{d\chi_{ij}}{dt}=\left(\sum_{kl}p_k^c\frac{\partial U_{ik}}{\partial\beta_l}\chi_{lj}+\sum_k U_{ki}\psi_{kj}\right)+\{i\rightleftharpoons j\}\,. \tag{2.7c}$$

Here $C_{ij}=\partial^2V/\partial\beta_i\partial\beta_j$, and the functions C, R, and U are all to be evaluated at the classical values $\beta_i=\beta_i^c$. The previously omitted term is the term containing $\partial R/\partial\beta$ in Eq. (2.7a). [There are also several factors of $\frac{1}{2}$ which were omitted[15] from Eqs. (10), (11), and (13) of Ref. 5.]

Equation (2.7) can be thought of as written for four degrees of freedom, where the first three are the shape coordinates and the fourth is the rotation angle.

The above equations are homogeneous in ω, ψ, and χ, except for the temperature term; so if the distribution does not have any width initially, the width will evolve only when there is a nonzero temperature.

In deriving Eq. (2.7) one makes use at various stages of the narrowness of the distribution. One retains only second order terms in $(p-p^c)$ and/or $(\beta-\beta^c)$. Also one drops boundary terms in the integration by parts, assuming that, even if the coordinates β have a finite domain, the distribution function still vanishes at the boundaries.

Once the second moments of the distribution are found, given the assumption of a narrow distribution, it follows that the form of W is Gaussian. Again following Ref. 5, if a matrix is constructed out of the submatrices ω, ψ, and χ,

$$A^{-1}=\begin{bmatrix}\omega & \psi\\ \psi & \chi\end{bmatrix}$$

and a column vector is constructed out of vectors p and β,

$$X=\begin{bmatrix}p\\ \beta\end{bmatrix}$$

then W is given by

$$W = (4\pi)^{-n}\Delta^{-1/2}\exp(-\tfrac{1}{4}X^{T}AX)\,, \qquad (2.8)$$

where $\Delta = \det(A^{-1})$, and n is the number of coordinates. (Actually one must take the determinant of the symmetric part of A^{-1}, which is what remains in the quadratic form.) It is possible to derive Eqs. (2.7) directly by placing the form of Eq. (2.8) into Eq. (2.5) and showing that the partial differential equation holds only if the ω, ψ, and χ obey Eq. (2.7). The distribution W is normalized to unity as written.

If one wants, for example, to find the distribution in just one variable, for example β_i, then one can integrate over all the other β's and the p's to find

$$w(\beta_i) = (4\pi\chi_{ii})^{-1/2}\exp\left[-\frac{(\beta_i-\beta_i^{\circ})^2}{4\chi_{ii}}\right].$$

More generally one might want to find a joint distribution function for a set of quantities $y_1, \ldots, y_k$ ($k \leq 2n$) which are known as functions of the p's and β's. This distribution is discussed in the Appendix.

Although there is some friction in the initial phase, in this model, and hence a nonzero temperature, we neglect fluctuations in the calculation of this early phase. Fluctuations begin with the deep phase and continue until the scission point. Some complications occur because the scission time t_{sc} is determined by a criterion

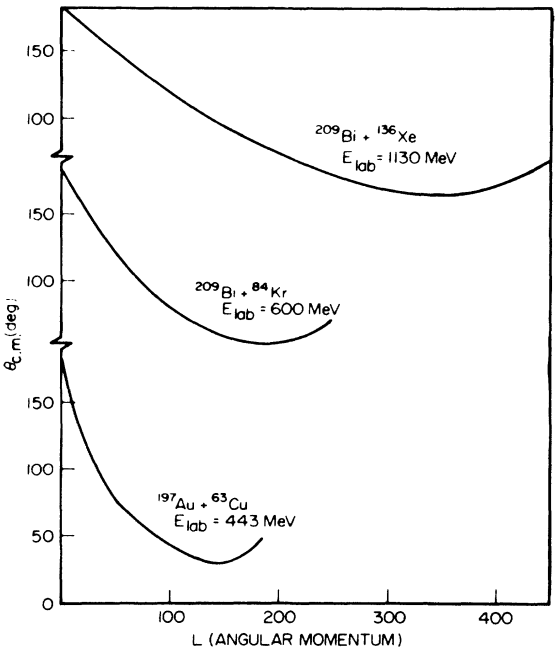

FIG. 1. Scattering angle (deflection function) for (^{209}Bi + ^{136}Xe), (^{209}Bi + ^{84}Kr), and (^{197}Au + ^{63}Cu) reactions at laboratory bombarding energies 1130, 600, and 443 MeV, respectively.

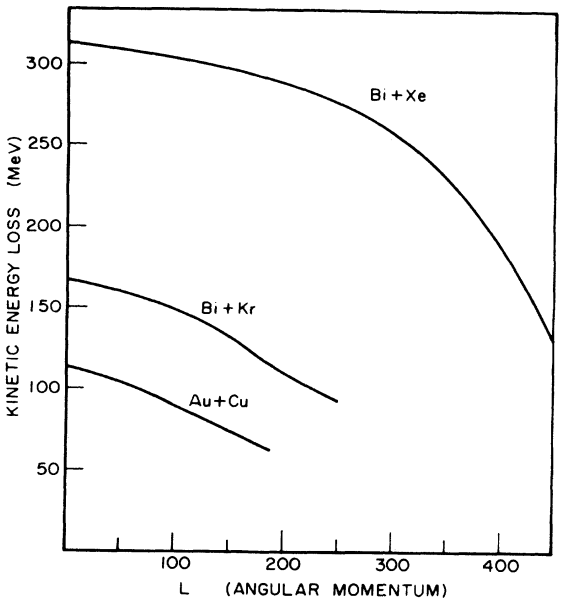

FIG. 2. Kinetic energy loss versus incident angular momentum for the reactions as in Fig. 1.

given in terms of the coordinates. Since the coordinates have a distribution, there will also be a distribution in t_{sc}. Thus, if we ask for the distribution at scission of a given quantity, for example θ, the rotation angle, then the width $\Delta\theta$ is determined by two quantities: (a) the width in θ that has evolved up to t_{sc}, and (b) the width Δt_{sc}. Details are given in the Appendix.

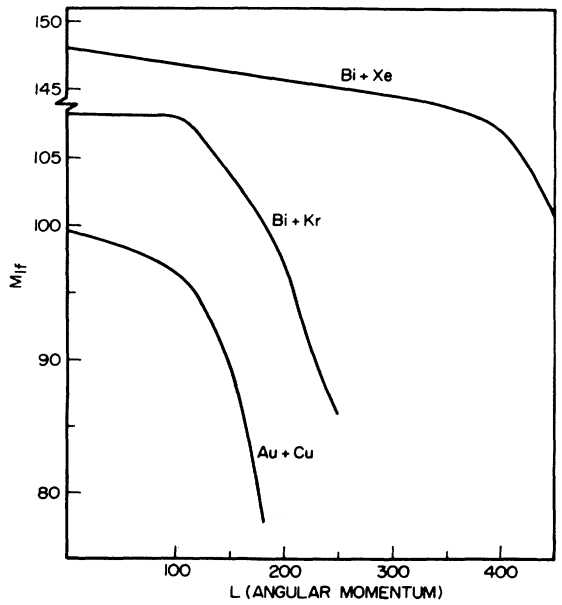

FIG. 3. Projectile-like final fragment mass versus incident angular momentum for the reactions as in Fig. 1.

III. RESULTS AND DISCUSSION

The model described in the previous section has been used to calculate experimentally observed quantities: angular, mass, and energy distributions for the reactions $^{209}Bi + ^{84}Kr$, $^{209}Bi + ^{136}Xe$, and $^{197}Au + ^{63}Cu$ at laboratory bombarding energies 600, 1130, and 443 MeV, respectively.[6-8] The deflection function, energy loss, and final mass of the projectile-like fragments are shown in Figs. 1–3. The results for Kr and Xe induced reactions are taken from Ref. 4, and represent the first moments of the distributions for these variables. They are the predictions of the classical, nonstatistical theory calculated for incident angular momentum from 0 to L_{max}, where L_{max} is the maximum angular momentum which can reach the distance r_{coll}. The kinetic model is used in all the calculations. The parameter h, the initial neck radius, is chosen so that the minimum of the deflection function occurs near the experimentally observed peak in the angular distribution, as discussed in Ref. 4. In this way the calculated cross section $d\sigma/d\theta$ has a maximum at this angle. It is shown in Ref. 4 that this maximum shifts toward more forward angles with the increase of the initial neck radius. We have used for h values of 4.9, 3.5, and 3.0 fm for the Xe, Kr, and Cu induced reactions, respectively. We note from the deflection function that our model predicts no fusion for any of the systems considered here.

In Figs. 4–6 we show the second moments of the scattering angle θ, final kinetic energy E_f, and final mass M of the projectile-like fragment as a function of incident angular momentum L. We have plotted σ_{xx} versus L (with $x = \theta$, E_f, or M), where $\sigma_{xx} = \sqrt{\chi_{xx}}$.

As outlined in the previous section, the final width is determined by two factors: (i) the intrinsic width caused by fluctuations developing up to the time of scission, and (ii) the width t_{sc} in the scission time. This latter turns out to be about one-fourth of the reaction time and broadens the width considerably. In particular we observe that the intrinsic width for E_f or M is comparable to

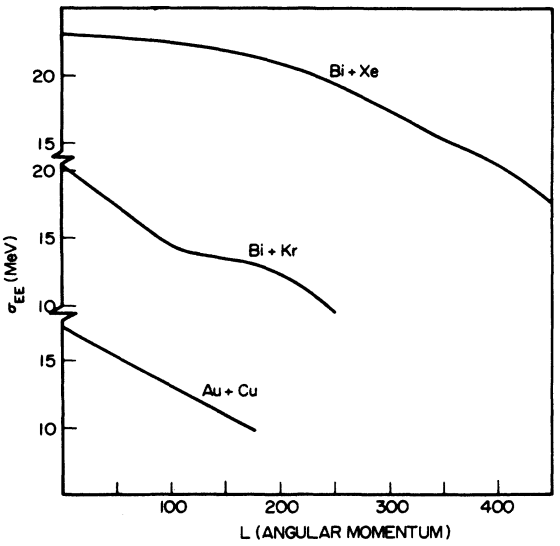

FIG. 5. Second moment for energy loss (variance $=2\sigma_{EE}^2$) for the reactions as in Fig. 1.

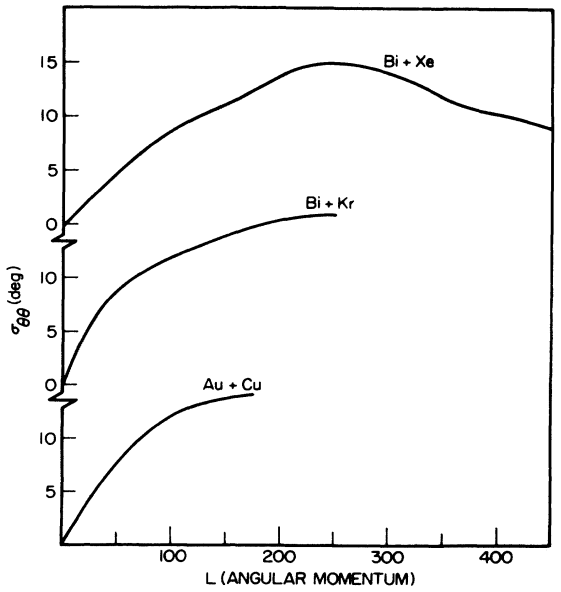

FIG. 4. Second moment for scattering angle (variance $=2\sigma_{\theta\theta}^2$) for the reactions as in Fig. 1.

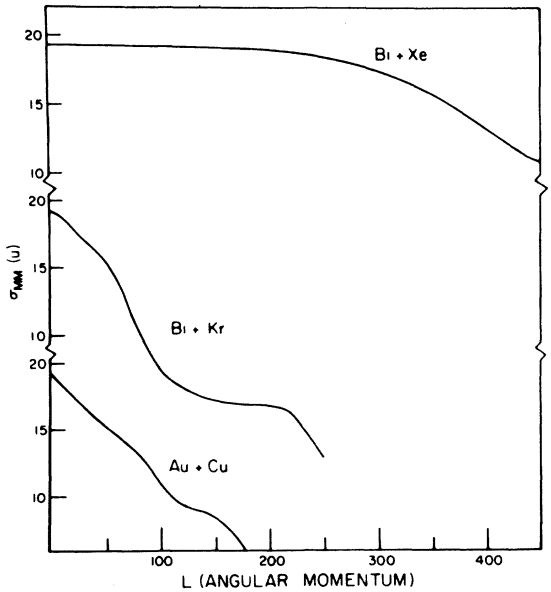

FIG. 6. Second moment for final mass (variance $=2\sigma_{MM}^2$) for the reactions as in Fig. 1.

the final width, but the intrinsic width for θ is an order of magnitude less than the total width. The intrinsic width in the rotation angle θ vanishes for head-on collision as shown below. Since in the collective phase $R_{4i}=R_{i4}=0$ for $i=1$ to 4 (this is due to angular momentum conservation, specifically the total angular momentum is conserved if, and only if, $\dot{L}=\dot{P}_4=(d/dt)(\partial\mathfrak{L}/\partial\dot{\theta})=R_{41}\dot{\beta}_1+R_{42}\dot{\beta}_2+R_{43}\dot{\beta}_2+R_{44}\dot{\theta}=0$ identically since θ is a cyclic coordinate) and $T_{4i}=T_{i4}=0$ for $i=1$ to 3, it can be seen from Eq. (2.7) (remembering that the stiffness tensor C, the friction tensor R, and the inverse inertia tensor U are independent of θ) that ω_{i4}, ω_{4i}, and ψ_{4i} $(i=1,2,3,4)$ satisfy a closed set of first order homogeneous differential equations. As the initial values of ω_{i4}, ω_{4i}, and ψ_{4i} vanish, they have zero value at all time. From Eq. (2.7c) we find that for $i=j=4$, the second term on the right hand side drops out and that $d\chi_{44}/dt$ is proportional to p_4 which is the angular momentum L. Thus for $L=0$, the intrinsic part of the fluctuation in θ, χ_{44}, $\sigma_{\theta\theta}{}^2=0$. The contribution to $\sigma_{\theta\theta}$ due to fluctuation in scission time is given by $\Delta t_{sc}\dot{\theta}_{sc}$, where $\dot{\theta}_{sc}$ is the angular velocity of the system at the classical scission point. Since for $L=0$, $\dot{\theta}_{sc}=0$, the total width in scattering angle vanishes for head-on collision. Now Δt_{sc} decreases as the incident angular momentum increases; but $\dot{\theta}_{sc}$ increases. This explains why $\sigma_{\theta\theta}$ starts with the value of zero, attains maximum, and then decreases, for

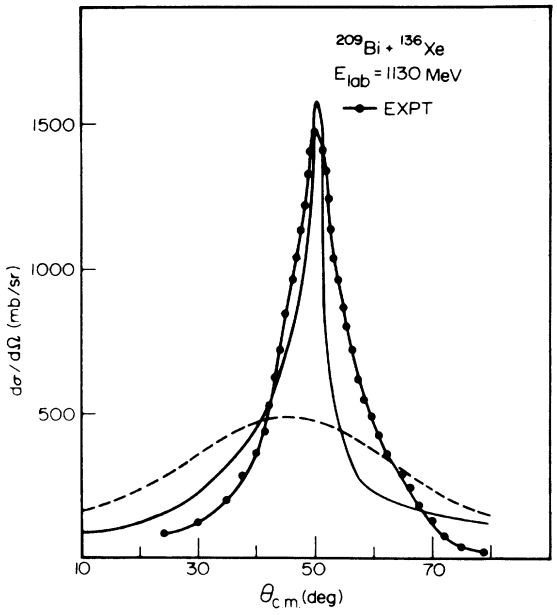

FIG. 7. Angular distribution for (Bi + Xe) reaction: The solid line with circles represents the experimental result; the dashed line corresponds to calculation using Model I; the solid line shows the calculation under Model II.

TABLE I. Maximum angular momentum L_{max} taking part in damped collisions, and the maximum angular momentum L_d going into the calculated deep phase.

System	E_{lab}(MeV)	L_d	L_{max}
Bi + Xe	1130	375	450
Bi + Kr	600	200	250
Au + Cu	443	125	175

the Xe induced reaction. (For the Kr and Cu induced reactions only the maximum is reached as L increases.) The other two widths $\sigma_{E_fE_f}$ and σ_{MM} are monotonically decreasing functions of L.

In Fig. 7 we compare the calculated angular distribution with experiment for the reaction Bi + Xe. The dashed line is our first calculation and the solid line with circles represents the experimental result. We observe that the calculated distribution is significantly broader than the experimental distribution.

We find that if all L's enter the deep phase we get distributions broader than observed distributions (in particular for the scattering angle). Up to this point we assumed that system always enters the collective phase if the ions reach the distance r_{coll}, that is, for L's up to L_{max}. It seems likely, however, that not all these L's enter the collective phase, forming a neck and undergoing shape changes as described above. Therefore, we now assume that the system does not enter the deep phase unless r reaches the value of R_1+R_2, the sum of the radii of the nuclei. This gives us, for each system, a quantity L_d, the maximum value of L which reaches the deep phase, which is smaller than the previously used L_{max}. Table I lists these values of L.

The reaction is thus divided into two parts: one for $L=0$ to $L=L_d$, treated as we have discussed, and one for L_d to L_{max}, to be treated by a more peripheral model. We note also that such a division is necessary in order to obtain the high energy part of the spectrum, since formation of the deep phase produces an energy loss $\geq$100 MeV, even for the maximum angular momentum.

For trajectories from L_d to L_{max} the appropriate degrees of freedom are r and θ, but it is clear that mass transfer continues to play a role in these more peripheral processes. In principle, one could carry out calculations of thermal fluctuations for r, θ, and mass asymmetry coordinates. Instead of this we have decided to use (only for these higher L's) the stochastic model used earlier by De *et al.*,[3] based on classical trajectories of r and θ, and random transfers of nucleons between the ions. We call this hybrid calculation, with collective coordinates used only for

L's from 0 to L_d, Model II. The original model, with collective coordinates used for all L's, will be called Model I.

Model II produces widths in θ significantly smaller than Model I. The calculation with Model II is shown by the solid line in Fig. 7. We observe that the width for Model II is in better agreement with experiment; in fact, it is somewhat too small. On the other hand, the widths in E_f and M are not very different for the two models.

Before discussing the mass distributions we observe that our model allows calculation of the final mass only. For the Bi + Xe reaction, only the charge distribution is measured. Therefore we use the relation $\sigma_{zz}^2 = (Z/A)^2\sigma_{AA}^2$, which is consistent with the strong correlation between neutron and proton transfer. This correlation is discussed in Ref. 13, and there is experimental evidence[16] that it is valid for large energy loss.

In Model II, when the stochastic calculation is used, the width of the charge distribution for the peripheral trajectories is determined directly.

In Fig. 8 we have compared the calculated charge distribution with experiment. The dashed line corresponds to Model I and the solid line corresponds to Model II. We note that for both cases, though the calculated widths are somewhat large as compared with experiment, the agreement is good. In Fig. 9 we display the kinetic energy distribution for various atomic numbers (labeled at each line) of the projectile-like fragments. The dashed and solid lines have the same meaning as in Fig. 8. We note that Model I gives significantly low cross sections as compared with experiment for small mass transfer and small energy loss.

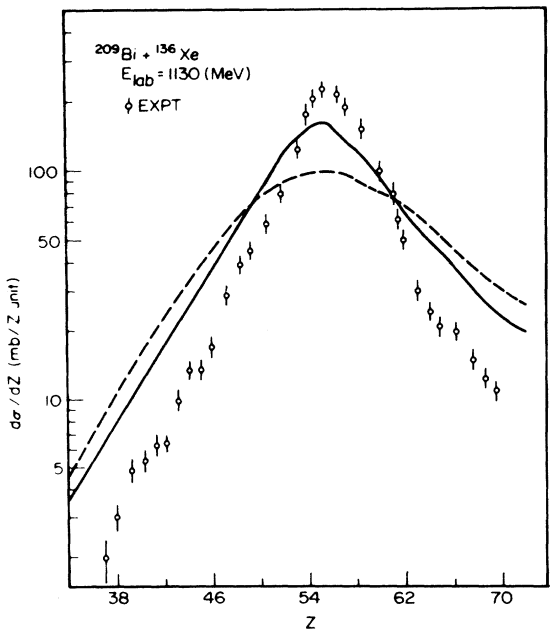

FIG. 8. Z distribution of projectile-like fragments for (Bi + Xe) reaction. The dashed line corresponds to calculation under Model I and the solid line represents the calculation with Model II.

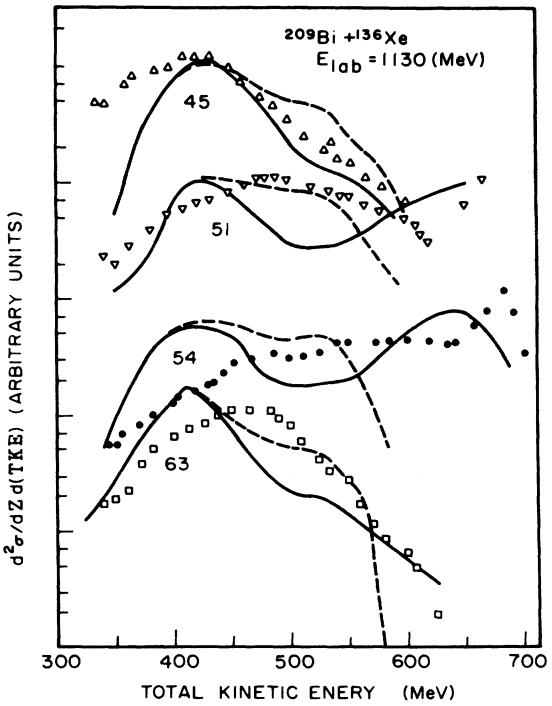

FIG. 9. Relative yield for fragments with fixed Z (as labeled at each curve) versus final total kinetic energy. Notations are the same as in Fig. 8.

The calculation of Model II shows dips at around 500 MeV final kinetic energy. This is an artifact of the model, due to the sharp transition, at $L = L_d$, from the collective calculation (using the deep phase) to the stochastic calculation.

In Fig. 10 we show the angular distributions of projectile-like fragments belonging to different energy groups—using Model II. The low cross section for the 525 MeV energy group is again due to the sharp transition from the collective to non-collective model. The basic feature that the widths of the distributions decrease with increasing final kinetic energy is well reproduced.

In Fig. 11 the angular distribution for the ^{209}Bi + ^{84}Kr reaction at $E_{lab} = 600$ MeV is shown. The same comments as in the case of the Xe induced reaction are also applicable here. In Fig. 12 we show the mass distribution of the Bi + Kr reaction for $\theta_{lab} = 34°$ and 59°. The basic features that for the larger scattering angles the mass transfer is greater and that the peak to valley ratio is greater are well reproduced. The calculated most probable mass transfer is about 5 units more than the

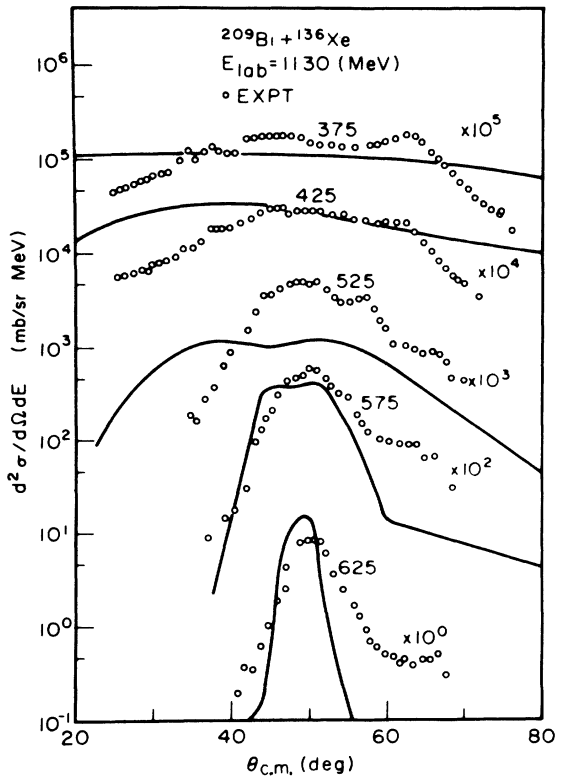

FIG. 10. Angular distribution for different fixed final kinetic energy under Model II.

experimental value for both scattering angles. In Fig. 13 we show the calculated mass distribution for the Kr induced reaction. The calculated most

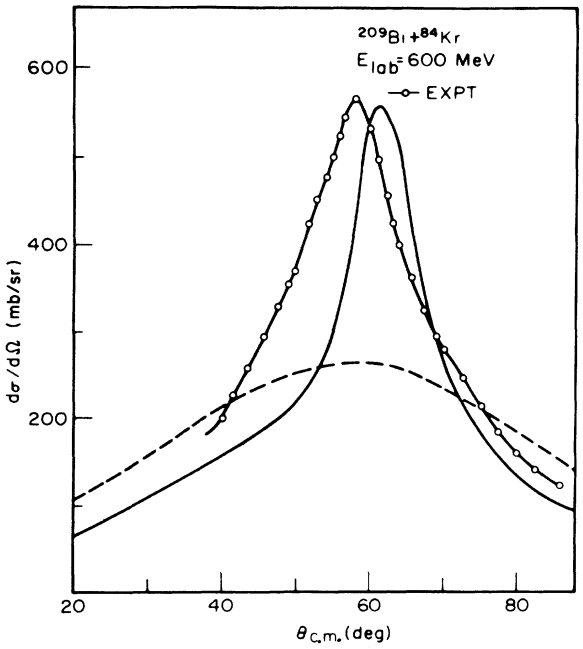

FIG. 11. Same as in Fig. 7 for the reaction (Bi + Kr).

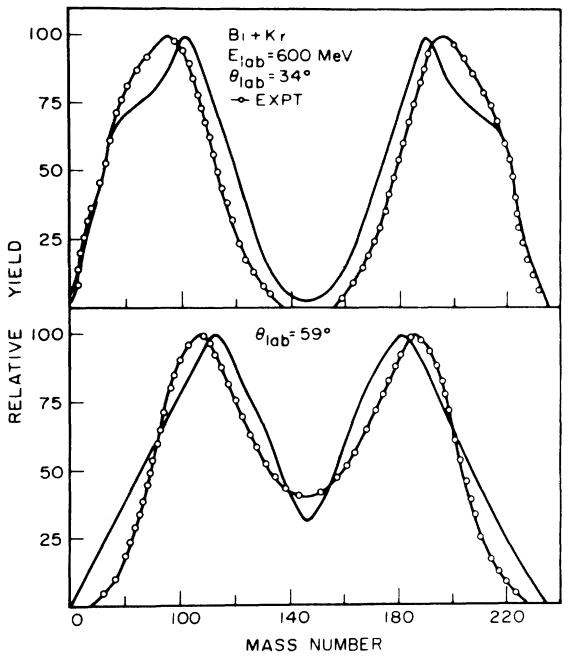

FIG. 12. Relative yield of various mass fragments for fixed scattering angle. The upper curve is for θ_{lab}=34° and the lower curve for θ_{lab}=59°; the calculation is performed under Model II.

probable mass transfer is about 5 units larger for Model I (dashed line) than for Model II (solid line).

In Fig. 14 the angular distribution for the Au + Cu

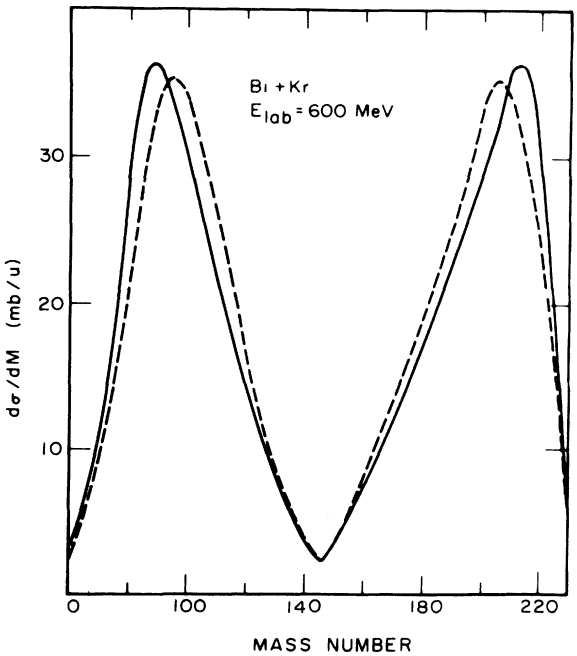

FIG. 13. Calculated cross section for various final fragment mass for Bi + Kr reaction. The dashed curve corresponds to Model I and the solid curve to Model II.

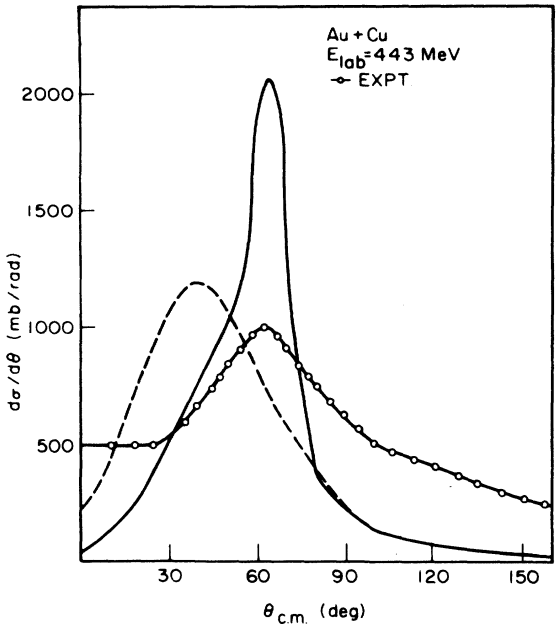

FIG. 14. Same as in Fig. 7 for (Au+Cu) reaction.

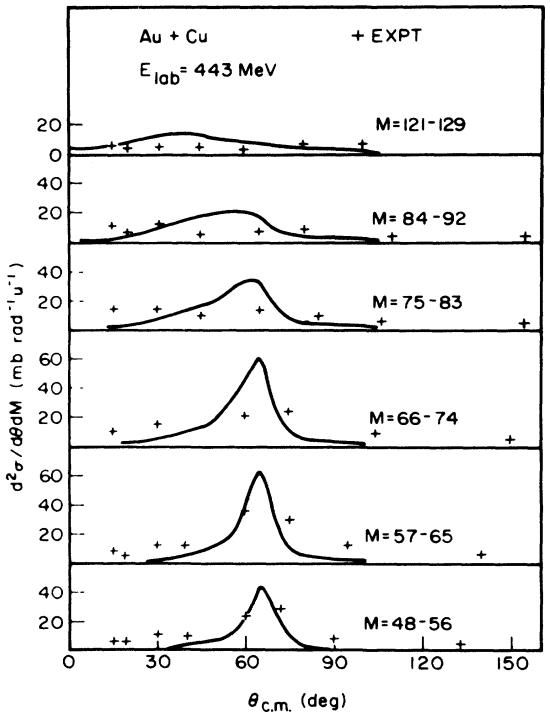

FIG. 15. Angular distribution for various mass groups for (Au+Cu) reaction with Model II.

reaction at $E_{lab}=443$ MeV is shown. Model I (dashed line) predicts peaking at too forward an angle as compared with experiment. It may be noted that the initial neck radius used corresponds to h_{min} for $L=L_{max}$. The peak is at the right position for Model II, but the distribution is too narrow. There is some evidence[8] for negative angle scattering for this reaction, but our calculation does not indicate any such scattering. In order to get negative angle scattering the conservative force must be taken to be more attractive, for example, by increasing the radius parameter. In this paper we have used a radius parameter $r_0=1.17$ fm and have not considered any variation of it. (There is evidence in fusion calculations for some freedom in the choice of radius parameters.[17]) Moreover, we mention that the calculation of the classical path is sensitive to the conservative forces, which we have assumed to be angular momentum independent (apart from the centrifugal force). In reality the forces depend on the excitation energy of the system, hence on the angular momentum, and this dependence will have some influence on the dynamics.

In Fig. 15 we show the angular distribution for various mass groups for the Au + Cu reaction. The experimental observations that the angular distribution is peaked near the grazing angle for masses around the projectile mass and that this peaking flattens out as one moves away from this mass are well reproduced. The flattening, however, is somewhat less than seen in the experimental data. Finally, in Fig. 16 we show the calculated mass distribution for this reaction.

In summary, we conclude that thermal fluctuations during the deep phase of strongly damped

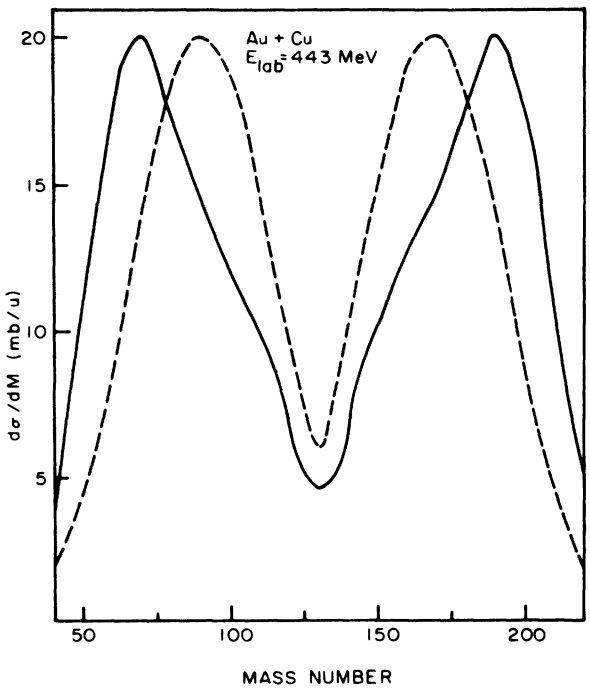

FIG. 16. Same as in Fig. 13 for (Au+Cu) reaction.

collisions are capable of reproducing the widths of the observed distributions in mass, energy, and angle. If one assumes that all the trajectories which are damped enter a deep (collective) phase, then the calculated widths, especially for the angular distribution, are too large. Also one obtains no cross section with relatively small energy loss (<100 MeV). On the other hand, if one assumes that some of the peripheral trajectories do not enter the collective phase, the predicted distributions are in agreement with experiment.

ACKNOWLEDGMENTS

One of us (M.I.S.) would like to acknowledge the hospitality of the Institut de Physique Nucléaire at Orsay, where part of this work was done, and also to acknowledge a helpful conversation with C. Ngô. Another one (S.K.S.) would like to gratefully acknowledge the hospitality of Brooklyn College, where a considerable part of this work was done, and also to acknowledge the financial support from the Research Foundation of the City University of New York. The author (S.I.A.G.) would like to acknowledge the hospitality of Rensselaer Polytechnic Institute, Troy, New York, where a part of this work was done. This work was supported by a PSC-BHE grant from the City University of New York and the United States Department of Energy.

APPENDIX

We consider a system described by parameters $x_1, x_2, \ldots, x_\nu$, where the x's may stand for coordinates and momenta. The system is described by a probability distribution $W(x_1, x_2, \ldots, x_\nu; t)$ at time t. If this system undergoes scission (or some other event which causes it to be described subsequently by a different set of coordinates) at time t_{sc}, the question is: What is the distribution at scission, $W_{sc}(x_1, x_2, \ldots, x_\nu)$? The time, t_{sc} is determined by a condition on the coordinates, which can be written in the form

$$\phi(x_1, \ldots, x_\nu) = 0 .$$

We are restricted to the case of narrow distribution, wherein W is a Gaussian and the widths of distributions are small. Then there is a Gaussian distribution in the scission time:

$$p(t_{sc}) = \frac{1}{\sqrt{4\pi}\,\Delta t_{sc}} \exp\left[-\left(\frac{t_{sc} - t_{sc}^c}{\Delta t_{sc}}\right)^2\right]. \tag{A1}$$

The superscript c refers to quantities evaluated for the classical path (or first moment of the distribution). t_{sc}^c is given by solving

$$\phi[x_1^c(t_{sc}^c), \ldots, x_\nu(t_{sc}^c)] = 0 .$$

The width Δt_{sc} is given by

$$\Delta t_{sc} = \Delta\phi / \dot{\phi}(t_{sc}^c) , \tag{A2}$$

where

$$\dot{\phi} = \sum_j \frac{\partial\phi}{\partial x_j}\,\dot{x}_j^c ;$$

the $\partial\phi/\partial x_j$ are evaluated at $x_j x_j^c$, and all the x and $\dot{x}$ are evaluated to t_{sc}^c. The quantity $\Delta\phi$ is the width in ϕ given the width of the x_j's at t_{sc}^c. The calculation of such quantities is discussed in the latter part of this Appendix.

The distribution at scission is now given simply by the folding

$$W_{sc}(x_1, \ldots, x_\nu) = \int dt_{sc}\, W(x_1, \ldots, x_\nu; t_{sc}) p(t_{sc}) . \tag{A3}$$

Now let W be given by

$$W = \left[\frac{\det A}{(4\pi)^\nu}\right]^{1/2} \exp\left\{-\tfrac{1}{4}\sum_{ij}[x_i - x_i^c(t)][x_j - x_j^c(t)]A_{ij}\right\}, \tag{A4}$$

where the A_{ij} are time dependent, as in Sec. II. Integrating over t_{sc} explicitly, we find W_{sc} takes the form

$$W_{sc} = \left[\frac{\det A_{sc}}{(4\pi)^\nu}\right]^{1/2} \times \exp\left\{-\tfrac{1}{4}\sum_{ij}[x_i - x_i^c(t_{sc}^c)][x_j - x_j^c(t_{sc}^c)]A_{sc,ij}\right\}. \tag{A5}$$

The matrix A_{sc} is given by

$$A_{sc,ij} = A_{ij} - \frac{\Delta t_{sc}^{\,2}}{1 + \Delta t_{sc}^{\,2}\sum_{kl}\dot{x}_k^c \dot{x}_l^c A_{kl}} \times \left(\sum_k \dot{x}_k A_{ik}\right)\left(\sum_l \dot{x}_l A_{lj}\right), \tag{A6}$$

where the $\dot{x}$ and the A are evaluated on the classical path at t_{sc}^c. As a special case we have, for one coordinate x,

$$\frac{1}{A_{sc}} = \frac{1}{A} + \dot{x}^2 \Delta t_{sc}^{\,2} .$$

Once the distribution at scission is known we may calculate the distribution in closed form at $t = +\infty$ since only the Coulomb force acts after scission. Thus the various quantities, such as the final kinetic energy, scattering angle, and mass, are given in closed form as functions of these quantities at scission.

We wish to determine, in general terms, the

distribution of a set of quantities, $y_1, y_2, \ldots, y_\mu$ which are functions of the x's, with $\mu \leq \nu$. We again treat deviations from the classical path to lowest order, letting

$$y_i = y_i^c + \sum_j \frac{\partial y_i}{\partial x_j}(x_j - x_j^c),$$

the partial derivatives evaluated on the classical path. Let us introduce the transformation matrix

$$\gamma_{ij} = \left(\frac{\partial y_j}{\partial x_i}\right)^c$$

(which need not be a square matrix). We may find the distribution in y by multiplying W by factors

$$\prod_{i=1}^{\mu} \delta\left(y_i - y_i^c - \sum_j \gamma_{ij}(x_j - x_j^c)\right),$$

and integrating over all the x's. By diagonalizing A this procedure is carried out explicitly, and we find the following simple result. If B is a $\mu \times \mu$ matrix given by

$$(B^{-1})_{ij} = \sum_{kl} \gamma_{ki}(A^{-1})_{kl}\gamma_{lj},$$

then the distribution in y, $\tilde{W}(y_1, \ldots, y_\mu)$, is given in terms of the elements of B, as

$$\tilde{W} = \left[\frac{\det B}{(4\pi)^\mu}\right]^{1/2} \exp\left[-\tfrac{1}{4}\sum_{ij}(y_i - y_i^c)(y_j - y_j^c)B_{ij}\right].$$

---

*On leave from Presidency College, Calcutta, India.
†On leave from Institute of Nuclear Research, Warsaw, Poland.

[1]J. P. Bondorf, M. K. Liou, M. I. Sobel, and D. Sperber, Nuovo Cimento 42A, 1 (1977); E. Seglie, A. Sherman, and D. Sperber, Phys. Rev. C 11, 1227 (1975); J. N. De, D. H. E. Gross, and H. Kalinowski, Z. Phys. A 277, 385 (1976); F. Beck, J. Blocki, M. Dworzecka, and G. Wolschin, Phys. Lett. 76B, 35 (1978); J. P. Bondorf, J. R. Huizenga, M. I. Sobel, and D. Sperber, Phys. Rev. C 11, 1265 (1975).
[2]W. Nörenberg, Phys. Lett. 53B, 289 (1974).
[3]A. Sherman, D. Sperber, M. I. Sobel, and J. P. Bondorf, Z. Phys. A 286, 11 (1978); J. N. De and D. Sperber, Phys. Lett. 72B, 293 (1978); J. N. De, S. I. A. Garpman, D. Sperber, and K. Tam, *ibid.* 76B, 39 (1978); J. N. De, S. I. A. Garpman, A. Sherman, D. Sperber, and K. Tam, *ibid.* 78B, 13 (1978).
[4]S. K. Samaddar, M. I. Sobel, J. N. De, S. I. A. Garpman, D. Sperber, M. Zielinska-Pfabe, and S. Møller, Nucl. Phys. A332, 210 (1979).
[5]C. Ngô and H. Hofmann, Z. Phys. A 282, 83 (1977).
[6]K. L. Wolf, J. P. Unik, J. R. Huizenga, J. R. Birkelund, H. Freisleben, and V. E. Viola, Phys. Rev. Lett. 33, 1105 (1974).
[7]J. R. Huizenga, J. R. Birkelund, W. U. Schröder, K. L. Wolf, and V. E. Viola, Jr., Phys. Rev. Lett. 37, 885 (1976); W. U. Schröder, J. R. Birkelund, J. R. Huizenga, K. L. Wolf, and V. E. Viola, Jr., Phys. Rep. 45, 301 (1978).
[8]C. Ngô, J. Peter, B. Tamain, M. Berlanger, and F. H. Hanappe, Nucl. Phys. A267, 181 (1976); J. Peter, C. Ngô, F. Plasil, B. Tamain, M. Berlanger, and F. Hanappe, *ibid.* A279, 110 (1977).
[9]J. Blocki, J. Randrup, W. J. Swiatecki, and C. F. Tsang, Ann. Phys. (N.Y.) 105, 427 (1977).
[10]J. Randrup, Ann. Phys. (N.Y.) 112, 356 (1978).
[11]S. K. Samaddar and M. I. Sobel, Phys. Lett. 88B, 43 (1979).
[12]K. T. R. Davies, R. A. Nanagan, J. R. Nix, and A. J. Sierk, Phys. Rev. C 16, 1890 (1977).
[13]S. K. Samaddar and M. I. Sobel, Phys. Lett. 82B, 191 (1979).
[14]S. Chandrasekhar, Rev. Mod. Phys. 15, 1 (1943); Donald A. McQuarrie, *Statistical Mechanics* (Harper and Row, New York, 1976), p. 459.
[15]C. Ngô (private communication).
[16]H. Breuer, B. G. Glagola, V. E. Viola, K. Wolf, A. C. Mignerey, J. R. Birkelund, D. Hilscher, A. D. Hoover, J. R. Huizenga, W. U. Schröder, and W. W. Wilcke, Phys. Rev. Lett. 43, 191 (1979).
[17]J. R. Birkelund, J. R. Huizenga, J. N. De, and D. Sperber, Phys. Rev. Lett. 40, 1123 (1978); J. R. Birkelund, L. E. Tubbs, J. R. Huizenga, J. N. De, and D. Sperber, Phys. Rep. 56, 108 (1979).